

## Photonic Technologies for Quantum Information Processing

Prem Kumar,<sup>1,7</sup> Paul Kwiat,<sup>2</sup> Alan Migdall,<sup>3</sup> Sae Woo Nam,<sup>4</sup>  
Jelena Vuckovic,<sup>5</sup> and Franco N. C. Wong<sup>6</sup>

*Received February 26, 2004; accepted May 6, 2004*

---

*The last several years have seen tremendous progress toward practical optical quantum information processing, including the development of single- and entangled-photon sources and high-efficiency photon counting detectors, covering a range of wavelengths. We review some of the recent progress in the development of these photonic technologies.*

---

**KEY WORDS:** Quantum dot; entanglement; down-conversion; single-photon detector.

**PACS:** 03.67.–a, 42.50.Dv, 42.65.Lm, 78.67.Hc, 85.60.Gz.

### 1. INTRODUCTION

It is now generally realized that fundamentally quantum-mechanical phenomena can enable significant, and in some cases, tremendous, improvement for a variety of tasks important to emergent technologies. Building on decades of successes in the experimental demonstration of such fundamental phenomena, it is not surprising that photonics is playing a

---

<sup>1</sup>Departments of Electrical and Computer Engineering, and Physics and Astronomy, Northwestern University, Evanston, Illinois 60208-3118, USA. E-mail: kumarp@northwestern.edu

<sup>2</sup>Department of Physics, University of Illinois, Urbana-Champaign, Illinois 61801-3080, USA.

<sup>3</sup>Optical Technology Div., NIST, Gaithersburg, Maryland 20899-8441, USA.

<sup>4</sup>Quantum Electrical Metrology Division, NIST, Boulder, Colorado 80305-3328, USA.

<sup>5</sup>Department of Electrical Engineering, Stanford University, Stanford, California 94305, USA.

<sup>6</sup>Research Laboratory of Electronics, MIT, Cambridge, Massachusetts 02139, USA.

<sup>7</sup>To whom correspondence should be addressed. E-mail: kumarp@northwestern.edu

preeminent role in this nascent endeavor. Many of the objectives of quantum information processing are inherently suited to optics (e.g., quantum cryptography<sup>(1)</sup> and optical metrology<sup>(2)</sup>), while others may have a strong optical component (e.g., distributed quantum computing<sup>(3)</sup>). In addition, it is now known that, at least in principle, one can realize *scalable* linear optics quantum computing (LOQC).<sup>(4)</sup> For these applications to attain their full potential, various photonic technologies are needed, including high fidelity sources of single and entangled photons, and high efficiency photon-counting detectors, both at visible and telecommunication wavelengths. Much progress has been made on the development of these, though they are still not up to the demanding requirements of LOQC. Nevertheless, even at their present stage they have direct application to initial experiments. Moreover, they may find use in various “adjacent” technologies, such as biomedical and astronomical imaging, and low-power classical telecommunications. Here we describe a number of the leading schemes for implementing approximations of sources of single photons on-demand and entangled photons, followed by a review of methods for detecting individual photons.

## 2. SINGLE-PHOTON SOURCES

Photon-based quantum cryptography, communication, and computation schemes have increased the need for light sources that produce individual photons. Ideally a single-photon source would produce completely characterized single photons on demand. When surveying attempts to create such sources, however, it is important to realize that there never has been and will never be such an ideal source. All of the currently available sources fall significantly short of this ideal. While other factors (such as rate, robustness, and complexity) certainly do matter, two of the most important parameters for quantifying how close a “single-photon source” approaches the ideal are the fraction of the time the device delivers light in response to a request, and the fraction of time that that light is just a single photon.

In general single-photon sources fall into two categories—isolated quantum systems, or two-photon emitters. The first type relies on the fact that a single isolated quantum system can emit only one photon each time it is excited. The trick here is obtaining efficient excitation, output collection, and good isolation of individual systems. The second type uses light sources that emit two photons at a time. Here the detection of one photon indicates the existence of the second photon. That knowledge allows the second photon to be manipulated and delivered to where it is needed.

## 2.1. Quantum Dot Single-Photon Sources

A quantum dot is essentially an artificial atom that is easily isolated, so it is an obvious choice as the basis of a single-photon source. Single photons on-demand have been generated by a combination of pulsed excitation of a single self-assembled semiconductor quantum dot and spectral filtering.<sup>(5)</sup> When such a quantum dot is excited, either with a short (e.g., 3 ps) laser pulse, or with an electrical pulse,<sup>(6)</sup> electron–hole pairs are created. For laser excitation, this can occur either within the dot itself, when the laser frequency is tuned to a resonant transition between confined states of the dot, or in the surrounding semiconductor matrix, when the laser frequency is tuned above the semiconductor band gap. In the latter case, carriers diffuse toward the dot, where they relax to the lowest confined states. Created carriers recombine in a radiative cascade, leading to the generation of several photons for each laser pulse; all of these photons have slightly different frequencies, resulting from the Coulomb interaction among carriers. The last emitted photon for each pulse has a unique frequency, and can be spectrally isolated.

If the dots are grown in a *bulk* semiconductor material,<sup>(6)</sup> the out-coupling efficiency is poor, since the majority of emitted photons are lost in the semiconductor substrate. To increase the efficiency, an optical microcavity can be fabricated around a quantum dot. An additional advantage is that the duration of photon pulses emitted from semiconductor quantum dots is reduced, due to an enhancement of the spontaneous emission rate. This enhancement, also known as the Purcell factor, is proportional to the ratio of the mode quality factor to the mode volume. In addition, the spontaneous emission becomes directional; the photons emitted into the nicely shaped cavity mode can be more easily coupled into downstream optical components.

By embedding InGaAs/GaAs quantum dots inside micropost microcavities with quality (Q)-factors of around 1300 and Purcell factors around five, the properties of a single-photon source have been significantly improved;<sup>(7)</sup> see Fig. 1. The probability of generating two photons for the same laser pulse [estimated from the zero-time correlation parameter  $g^{(2)}(0)$ ] can be as small as 2% compared to a Poisson-distributed source (i.e., an attenuated laser) of the same mean photon rate, the duration of single-photon pulses is below 200 ps, and the sources emit identical (indistinguishable) photons, as confirmed by two-photon interference in a Hong-Ou-Mandel type experiment.<sup>(7)</sup> Such sources have been employed to realize the BB84 QKD protocol, and to generate post-selected polarization-entangled photons.<sup>(8)</sup>

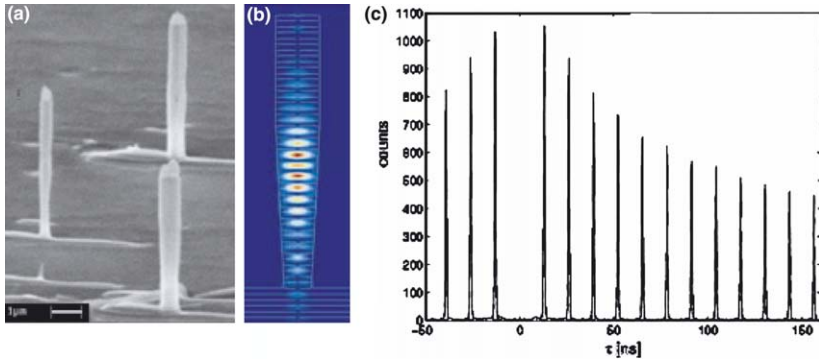


Fig. 1. (a) Scanning electron micrograph showing a fabricated array of GaAs/AlAs microposts ( $\sim 0.3\text{-}\mu\text{m}$  diameters,  $5\text{-}\mu\text{m}$  heights), with InAs/GaAs quantum dots embedded at the cavity center. (b) Electric field magnitude of the fundamental  $\text{HE}_{11}$  mode in a micropost microcavity with a realistic wall profile. (c) Photon correlation histogram for a single quantum dot embedded inside a micropost and on resonance with the cavity, under pulsed, resonant excitation. The histogram is generated using a Hanbury Brown and Twiss-type setup—the vanishing central peak (at  $\tau = 0$ ) indicates a large suppression of two-photon pulses (to  $\sim 2\%$  compared to a Poisson-distributed source, e.g., an attenuated laser, of the same intensity). The 13-ns peak-to-peak separation corresponds to the repetition period of excitation pulses.

These sources still face several great challenges, however. They require cryogenic cooling ( $< 10\text{ K}$ ), the output wavelengths are not yet readily tunable (present operation is around  $900\text{ nm}$ ), the out-coupling efficiency into a single-mode traveling wave is still rather low ( $< 40\%$ ),<sup>(9)</sup> and excitation of quantum dots in microcavities presently requires *optical* pumping (electrical pumping would be more desirable and efforts in that direction are underway<sup>(6)</sup>). In the future, photonic-crystal microcavities may lead to much higher ratios of the quality factor to mode volumes, and therefore, much stronger cavity QED effects should be possible.<sup>(10)</sup> This would enable an increase in the efficiency and speed of the single-photon devices, and thus open the possibility for building integrated quantum information systems. The spontaneous emission lifetime could be reduced further to on the order of several picoseconds, which would allow the generation of single photons at a rate higher than  $10\text{ GHz}$ . Moreover, the Purcell effect would also help in bringing the emitted photons closer to being Fourier-transform limited in bandwidth. Finally, photonic-crystal based cavities could even enable the realization of the strong coupling regime with a single quantum dot exciton, opening the possibility for the generation of completely indistinguishable single photons by coherent excitation schemes.

## 2.2. Other Single-Emitter Approaches

Other isolated quantum system approaches to producing single photons include isolated single fluorescence molecules<sup>(11)</sup> and isolated nitrogen vacancies in diamond.<sup>(12)</sup> Two significant deficiencies of these sources for many applications are that it is not easy to efficiently out-couple the photons, and that the spectral spread of the light is typically quite large ( $\sim 120$  nm), though widths as low as 12 nm have been seen in new results.<sup>(11)</sup> This spectral width is non-optimal for applications relying on two-photon interference effects, and also for quantum cryptographic applications (where one typically desires fairly narrow bandwidths to exclude background light).

More recently, single atoms<sup>(13)</sup> coupled to a high-finesse optical cavity have demonstrated features of single-photon operation. Despite the technological challenges, this approach does offer the large potential advantage that the photons are emitted preferentially into the cavity modes, which are easier to couple out of, with couplings of 40–70% already achieved. Also, the frequency of the photons is necessarily matched to a strong atomic transition, which may allow for efficient quantum *communication* using photons, while other quantum information processing tasks, such as memory or state readout, are carried out in the atomic system.<sup>(14,15)</sup>

## 2.3. Downconversion Single-Photon Sources

Another effort toward single-photon sources relies on producing photons in pairs, typically via the process of optical parametric down conversion (PDC).<sup>(16)</sup> The PDC process effectively takes an input photon from a pump beam and converts it into output pairs in a crystal possessing a  $\chi^{(2)}$  nonlinearity. Thus the detection of one photon can be used to indicate (or herald) the existence of the second photon, which is available for further use. This second photon is, at low photon rates, left in an excellent approximation to a single-photon number state.<sup>(17)</sup> It has been demonstrated how these photons may then be converted into completely arbitrary quantum states with fidelities of 99.9%.<sup>(18)</sup> Recent efforts have focused on improving the collection of those pairs and improving the “single-photon accuracy,” e.g., the value of  $g^{(2)}$  (0).

The physics of the PDC process guarantees that the output pairs will possess certain energy and momentum constraints, so that under appropriate conditions the detected location of the herald photon tightly defines the location of its twin, a significant advantage over other single-photon schemes. There have been many mode-engineering efforts to improve this collection into a *single* mode,<sup>(19)</sup> but the current best collection efficiency is

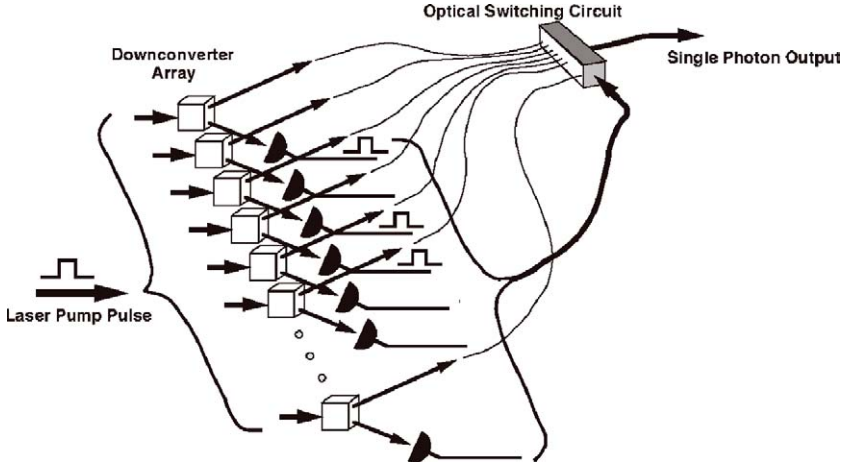


Fig. 2. Multiplexed PDC scheme to better approximate a source of single photons on demand. By operating an array of simultaneously pumped PDC sources at low photon production rates and optically switching the output of one of the PDC sources that *did* produce a photon to the single output channel, it is possible to increase the single-photon rate, while maintaining a low rate of unwanted multiphoton pulses.

still only 58%<sup>8</sup>, including 15% optical-transmittance losses. (Contrast this to the required single-photon efficiency of over 99% for LOQC.)<sup>(4)</sup> One example of a method to improve this is to directly modify the spatial emission profile of the photon pairs (which are usually emitted along cones) so that the photons are emitted preferentially into “beacon”-like beams, which couple more naturally into single-mode optical fibers.<sup>(20)</sup> Another approach yet to be explored is the use of adaptive optics to tailor the output modes. It should be noted that not all quantum information processing applications require single-mode performance; for example, free-space quantum key distribution is likely to work nearly as well with a small number of modes.

Because the conversion of pump photons into pairs via PDC is a random process, these sources suffer from the same problem that afflicts faint laser sources—one cannot guarantee that one and only one photon pair is created at a time (i.e.,  $g^{(2)}(0) \neq 0$ ). Multiplexing and storage schemes have been proposed to deal with this. They both work by similar principles (one scheme is based on space multiplexing<sup>(21)</sup>—see Fig. 2—and the other is based on temporal multiplexing<sup>(18,22)</sup>)—photons are created at relatively low rates where the probability of simultaneous multi-pair production is

<sup>8</sup>An 83% coupling efficiency has recently been reported. See quant-ph/0408093.

low; contingent on the detection of a herald photon, the twin is then “stored”, to be emitted in a controlled fashion at some later desired time. The overall emission rate is reduced, but the rate of producing one and only one photon at regular intervals is improved.

### 3. ENTANGLED-PHOTON SOURCES

Entangled states are now known to be a critical resource for realizing many quantum information protocols, such as teleportation and quantum networking. An on-demand source of entangled photons would also greatly aid the realization of all-optical quantum computing.

#### 3.1. Down-Conversion Schemes

At present, by far the most prevalent source of entangled photon pairs is parametric down conversion based on crystals with a  $\chi^{(2)}$  non-linearity. As discussed above, it is precisely the temporal and spatial correlations between the photon pairs which make them very promising for the realization of an on-demand source of single photons. Much of the effort in studying these sources has been devoted to the generation of *polarization*-entangled photon pairs, an area which has seen tremendous growth—more than a million-fold improvement in the detected rates of polarization-entangled photons has been achieved in the past two decades (see Fig. 3).

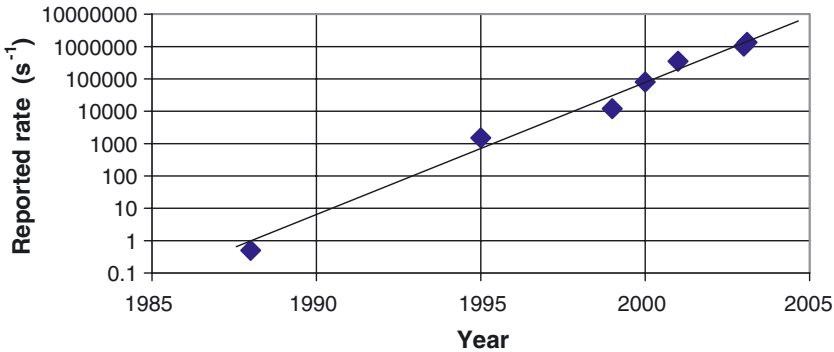


Fig. 3. The apparent “Moore’s Law” for entanglement. Shown are the reported detection rates of (polarization)-entangled photon pairs (from down conversion), as a function of year. The solid line—drawn to guide the eye—indicates the  $\times 100$  gain every 5 years. The primary limiting factor has now become the lack of single-photon counting detectors with saturation rates above 10 MHz.

There are now several ways to realize polarization entanglement using the PDC process. One method uses a single nonlinear crystal, cut for “type-II” phase matching, and selecting out a particular pair of output directions.<sup>(23)</sup> Although initially these sources used large gas lasers for pumping, the recent availability of ultraviolet diode lasers has led to much more compact sources.<sup>(24)</sup> A potentially important disadvantage, in addition to the need to compensate the birefringent walk-off with this scheme, is that the entanglement is present only over a particular pair of modes (corresponding to the intersection of two cones). One method to eliminate this disadvantage is to pump the crystal from two different directions,<sup>(25,26)</sup> or to allow the PDC to occur in either of *two* crystals, the outputs of which are superposed directly<sup>(27,28)</sup> or using a beam splitter.<sup>(29)</sup> By proper alignment, nearly all of the output modes can display polarization entanglement, which moreover is completely tunable.<sup>(30)</sup> Nearly perfect entanglement (within statistical uncertainty) has been observed with such sources. Results with short-pulse pumps<sup>(28,29,31)</sup> are encouraging, but the quality of the entanglement is typically not as high, a problem that will need to be addressed for future applications.

One disadvantage of all of these techniques is that the output spectral bandwidth is still quite wide (typically 1–10 nm) for possible coupling to atomic states. Research is underway to circumvent this problem by placing the nonlinear crystals inside high finesse optical cavities, which significantly increases the probability of downconversion into a narrow spectral bandwidth.<sup>(14)</sup>

As discussed above, there are a number of approaches for improving the coupling efficiency into single spatial modes. Improving conversion efficiency by finding higher non-linearity bulk crystals is limited by the choice of available crystals (with BBO and LiIO<sub>3</sub> being two of the better ones). Engineering crystals by processes such as periodic poling<sup>(32)</sup> allows one to take advantage of crystals (e.g., Lithium Niobate) with somewhat higher nonlinearities. The conversion efficiency into a specific mode can be further enhanced by some 1–2 orders of magnitude by creating waveguides in these crystals.<sup>(33)</sup> Because the waveguide is small, possibly even single mode, it can be much easier to collect the output light. However, the net outcoupling efficiencies achieved to date (10–20%) still require substantial improvement. Finally, by using a buildup cavity to recycle the unconverted pump photons, the effective conversion efficiency may be increased (at the expense of a more complicated setup).<sup>(34)</sup>

Entanglement in non-polarization degrees of freedom, such as energy/time-bin<sup>(35)</sup> and orbital angular momentum,<sup>(36)</sup> has also been realized recently. These may present some advantages over the polarization case, e.g., they allow implementation of higher-order quantum structures,



such as qu-trits (3-level systems), and timing entanglement is more robust for transmission through optical fibers.

One problem plaguing all of these sources is that the production of pairs is a random process. By using short pulsed pumps, it is possible to define the times when *no* photon pairs will be produced, but there is still no way to guarantee production of exactly one photon-pair during any given pulse. At least one theoretical scheme has been proposed to circumvent this problem,<sup>(37)</sup> but practical implementations have yet to be realized.

### 3.2. $\chi^{(3)}$ -Nonlinearity Schemes

The difficulty of coupling the entangled photons into optical fibers has been overcome by directly producing them *inside* of the fiber, by exploiting the  $\chi^{(3)}$  (Kerr) nonlinearity of the fiber itself.<sup>(38)</sup> By placing the pump wavelength close to the zero-dispersion wavelength of the fiber, the probability amplitude for inelastic four-photon scattering can be significantly enhanced. Two pump photons at frequency  $\omega_p$  scatter through the Kerr nonlinearity to create simultaneous energy-time-entangled signal and idler photons at frequencies  $\omega_s$  and  $\omega_i$ , respectively, such that  $2\omega_p = \omega_s + \omega_i$ . Because of the isotropic nature of the Kerr nonlinearity in fused-silica-glass fibers, the correlated scattered photons are predominantly co-polarized with the pump photons. Two such correlated down-conversion events from temporally multiplexed orthogonally polarized pumps can be configured to create polarization entanglement as well. In this way all four polarization-entangled Bell states have recently been prepared, violating Bell inequalities by up to ten standard deviations of measurement uncertainty.<sup>(39)</sup> One drawback is the existence of Raman scattering in standard optical fibers due to coupling of the pump photons with optical phonons in the fiber. However, for small pump-signal detunings the imaginary part of  $\chi^{(3)}$  in standard fibers is small enough that a 10-fold higher probability of creating a correlated photon-pair in a suitable detection window can be obtained than the probability of two uncorrelated Raman-scattered photons in the same detection window.<sup>(40)</sup> Further work to quantify Raman scattering at the single-photon level is needed.

### 3.3. Quantum Dot Entangled-Photon Sources

A biexcitonic cascade from a semiconductor quantum dot might also allow the generation of polarization-entangled photon pairs on demand, since the selection rules should translate the anticorrelation of electron and hole spins in the biexcitonic state into polarization anticorrelation of photons.<sup>(41)</sup> However, this requires that the two decay paths from the biexcitonic state

are indistinguishable; therefore, the effects such as dot anisotropy, strain, piezoelectric effects, and dephasing processes need to be minimized.<sup>(42)</sup> To accomplish this, one needs to optimize quantum dot growth conditions and employ novel high-Q photonic crystal microcavities, which would increase the radiative recombination rate over the dephasing rate.<sup>(43)</sup>

## 4. SINGLE-PHOTON DETECTORS

As noted in the introduction, photon-based quantum information processing applications require that single photons, or more generally, the photon number in a multiphoton state, be detected with efficiency approaching unity. To that end much progress has been made in recent years towards developing high efficiency, low noise, and high count-rate detectors, which can reliably distinguish the photon number in an incident quantum state.

### 4.1. Avalanche Devices

Detection of single photons with avalanche photodiodes<sup>(44)</sup> (APDs) biased above the breakdown voltage is convenient (no cryogenic temperatures are needed) and relatively efficient. When one or more photons are absorbed, the generated carriers that undergo avalanche gain may cause a detectable macroscopic breakdown of the diode p-n junction. APD photon counters suffer both from dark counts, where thermally generated charge carriers cause a detection event, and from after-pulses, where carriers from a previous avalanche cause subsequent detection events when the APD is reactivated.

The best counters at visible wavelengths have been made with silicon APDs. These work well because of both the material system's ability to provide very low-noise avalanche gain and the availability of silicon of nearly perfect quality. For example, the single-photon counting modules (SPCMs), made by Perkin-Elmer (SPCM-AQR-16), can have 50–70% quantum efficiency near 700-nm wavelength, dark-count rate < 25/s, and can count at rates up to 10–15 MHz.<sup>†(45)</sup> The dark-count rate is low enough for the SPCMs to be operated continuously except for a 50-ns avalanche quench time, although heating effects limit the CW counting rate to about 5 MHz. After-pulsing is less than 0.5%. The quantum efficiency of

---

<sup>†</sup>Certain trade names and company products are mentioned in the text in order to specify adequately the experimental procedure and equipment used. In no case does such identification imply recommendation or endorsement by the National Institute of Standards and Technology, nor does it imply that the products are necessarily the best available for the purpose.

the SPCMs drops at longer wavelengths (2% at  $1\ \mu\text{m}$ ). Attempts to resolve multiple photons by splitting a multi-photon pulse into several time bins (e.g., with a storage loop) have been made, but they are limited by losses in the device switching photons into and out of the loop, and by the non-unity detector efficiencies.<sup>(46)</sup>

The Visible Light Photon Counter<sup>(47)</sup> (VLPC) and Solid State Photomultiplier<sup>(48)</sup> (SSPM) are modified Si devices which operate using a spatially localized avalanche from an impurity band to the conduction band. They possess high quantum efficiency (estimated to be  $\sim 95\%$ ) with low multiplication noise. The localized nature of the avalanche allows high efficiency photon-number discrimination,<sup>(49)</sup> which is not possible with conventional APDs. Using this capability, the non-classical nature of PDC has been investigated and violations of classical statistics demonstrated.<sup>(50)</sup> Unfortunately, these detectors require cooling to 6 K for optimal performance, and even then they display dark count rates in excess of  $10^4\ \text{s}^{-1}$ .

In the infrared,  $1\text{--}1.6\ \mu\text{m}$ , the best results to date have come from APDs having InGaAs as the absorption region that is separate from a multiplication layer of InP<sup>(51)</sup>; see Fig. 4. This has proven to be a

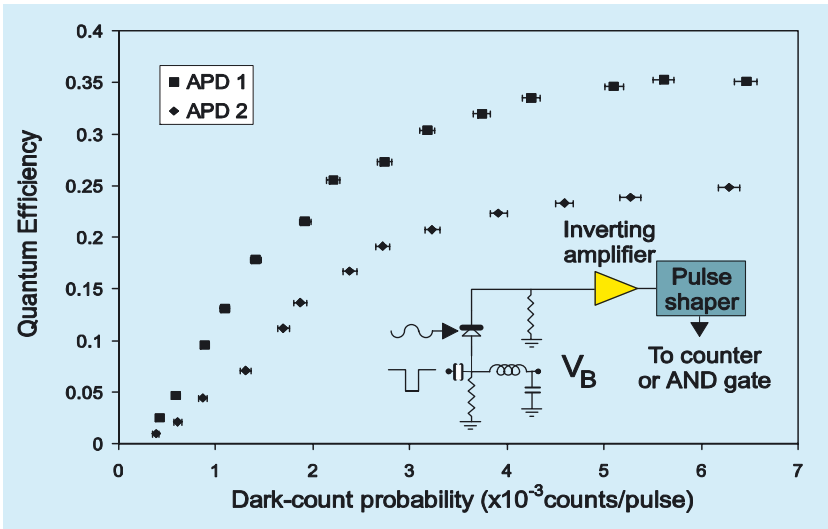


Fig. 4. Quantum efficiency versus dark-count probability for two InGaAs APDs operated in gated Geiger mode near  $1537\ \text{nm}$  wavelength. In the gated Geiger mode, the APD is biased below breakdown and a short electrical pulse ( $\sim 1\ \text{ns}$ ), coincident with the incident light pulse containing the photon to be detected, brings it momentarily into the breakdown region. The inset shows a schematic of the electronic circuit used with the APDs (from Ref. 38).

better solution than germanium APDs.<sup>(52)</sup> To suppress the high dark count rate in these devices, at best thousands of times worse than in silicon APDs, cooled InGaAs/InP APDs are usually activated for only  $\sim 1$ – $10$  ns duration to coincide with the arrival of the photon to be detected. The reported quantum efficiencies are typically between 10–30%, and the APDs are usually operated at a count rate of 100 kHz in order to alleviate after-pulsing caused by carriers trapped between the InGaAs and InP layers.

## 4.2. Superconducting Devices

Superconducting devices offer the potential to achieve levels of performance that exceed those of conventional semiconductor APDs. Although there are many types of superconducting detectors, only three have been used to observe single optical photons: the transition-edge sensor<sup>(53)</sup> (TES), the superconducting tunnel junction<sup>(54)</sup> (STJ), and the superconducting single-photon detector (SSPD).<sup>(55)</sup> Both the TES and the STJ detectors have been able to detect single photons and count the number of photons absorbed by the detector. The TES detector uses the steep slope of the resistance as a function of temperature at the superconducting transition as a very sensitive thermometer. This thermometer is able to measure the temperature change in an absorber when one or more photons are absorbed (see Fig. 5). The TES detectors are slow, capable of count rates at most up to 100 kHz, but essentially have no dark counts.<sup>(53)</sup> The reported detection efficiency currently varies from 20% to 40% in the telecom to optical band, although significant improvements in detection efficiency and speed are being realized with better detector designs (e.g., anti-reflection coatings) and research into new superconducting materials.

In an STJ detector, excitations of the superconductor are generated when a photon is absorbed. The excited quasiparticles can create an enhanced tunneling current which is proportional to the energy of the photon (or the number of photons absorbed). These detectors are similar in speed to the TES and also have no dark counts. The detection efficiency demonstrated to date is roughly 40% for visible photons,<sup>(54)</sup> which could be improved with AR coatings.

The SSPD detectors are extremely fast detectors ( $\sim 100$ -ps total pulse duration) that have single photon sensitivities.<sup>(55)</sup> In an SSPD, the detector is a narrow superconducting current path on a substrate. This path is current-biased at a point just below the superconducting critical current. A local hot spot is formed where a photon(s) is absorbed, locally destroying the superconductivity. This forces the current to flow around the hot spot

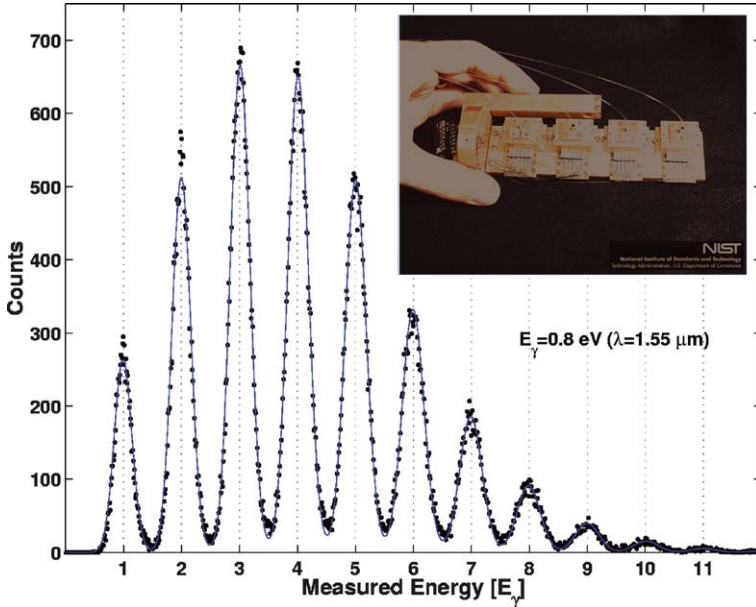


Fig. 5. Measured Poisson photon-number distribution of an attenuated, pulsed 1550-nm laser, repeatedly measured using a TES. The TES devices are made of superconducting tungsten and operated at a temperature of 100 mK. The horizontal axis is the pulse height of the photon absorption events in units of the energy of one 1550-nm photon, 0.8 eV (from Ref. 53). The inset shows a photograph of four fiber-coupled devices prepared to be cooled to 100 mK.

causing the current density around the hot-spot to exceed the critical current density. As a result, the device develops a resistance, causing a voltage to appear across the device. These detectors are single-photon-threshold devices and are not able to resolve the photon number in multiphoton pulses. Typical implementations use meandering paths to increase the sensitive area, which is otherwise very small due to the narrowness required for the conducting path. Much improvement in device fabrication and design is needed to improve the quantum efficiencies of these devices beyond the current values of ~20%; the detection efficiency is lower still, due to the area effect mentioned above.

### 4.3. Frequency Upconversion

Detection techniques based on frequency upconversion allow IR photons to be converted into the visible where single photon detection is more efficient and convenient. Frequency upconversion uses sum-frequency

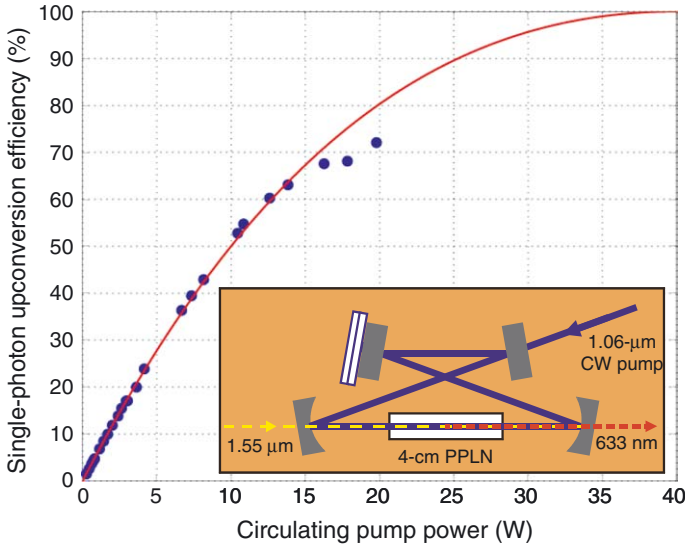


Fig. 6. CW single-photon upconversion efficiency versus circulating pump power in the pump enhancement ring cavity (inset). Solid line is a theoretical fit to data. At high pump powers lower than expected efficiencies are due to heating in PPLN that caused thermal instability in the ring cavity lock. See Ref. 56 for results with improved cavity lock.

generation in a non-linear optical crystal to mix a weak input signal at  $\omega_{\text{in}}$  with a strong pump at  $\omega_{\text{p}}$  to yield a higher-frequency output field at  $\omega_{\text{out}} = \omega_{\text{in}} + \omega_{\text{p}}$ . With sufficient pump power this upconversion can occur with near unity efficiency even for weak light fields at the single-photon level. For LOQC and quantum key distribution applications, telecommunication-wavelength photons at  $1.55 \mu\text{m}$  can then be efficiently detected with low-noise, high quantum-efficiency Si APDs. Recently, up-conversion of single photons from  $1.55$  to  $0.63 \mu\text{m}$  in bulk periodically poled lithium niobate (PPLN) has been demonstrated with an efficiency of 90%,<sup>(56)</sup> limited only by the available continuous wave (CW) pump power at  $1.06 \mu\text{m}$ , see Fig. 6. The bulk PPLN crystal is embedded inside a pump enhancement cavity that also imposes a well-defined spatial mode for the single-pass input photons. One approach to eliminate the need for a stabilized buildup cavity is to use a bright pulsed escort beam which is temporally mode-matched to the input photon. Such a system has enabled single-photon conversion efficiencies of  $\sim 80\%$  and backgrounds less than  $10^{-3}$  per pulse.<sup>(57)</sup>

The pump power requirement can be relaxed by using a waveguide PPLN crystal,<sup>(58)</sup> but the effect of waveguide losses must be addressed

to achieve the required near-unity net upconversion efficiency. The next step is to demonstrate frequency upconversion of a quantum state,<sup>(59)</sup> i.e., high fidelity frequency translation of a single photon in an arbitrary quantum polarization state. This will allow a modular approach to developing LOQC technologies. For example, the photonic qubits and ancilla photons can be prepared at wavelengths with the most convenient and efficient methods, and then converted with near-unity efficiency to wavelengths that are optimal for photonic logic gates employing quantum interference. Similarly, tunable quantum frequency upconversion can be used to match the required wavelengths to the resonant transitions in various atomic systems, for applications such as quantum repeaters.<sup>(14)</sup> As another example, there have also been proposals<sup>(15)</sup> to couple the photons to an atomic vapor system—the excitation of a single atom can be made very probable by having many atoms, and that excitation can be read out with very high efficiency by using a cycling transition. Such schemes could potentially yield efficiencies in excess of 99.9%. However, there are critical noise issues which must still be addressed.

## 5. CONCLUSIONS

For reasons noted in the introduction, there is intense current interest in creating robust, high-precision sources and detectors of single photons. In the last year alone, two special issues have appeared in the literature focusing just on these topics.<sup>(60,61)</sup> Though tremendous progress has been achieved, more development is clearly necessary to bring these technologies to the level of operation needed for LOQC. Nevertheless, already they have shown promise, enabling the realization of simple quantum gates, and improved quantum key distribution protocols. We anticipate that further improvements over the next few years will continue to make optical qubits an attractive system, though it remains to be seen whether the extremely demanding LOQC requirements can be met.

## ACKNOWLEDGMENTS

P. Kumar and F. Wong would like to acknowledge support of the MURI Center for Quantum Information Technology: Entanglement, Teleportation, and Quantum Memory (ARO program DAAD19-00-1-0177); P. Kwiat, A. Migdall, Sae Woo Nam, and J. Vuckovic would like to acknowledge support by the MURI Center for Photonic Quantum Information Systems (ARO/ARDA program DAAD19-03-1-0199). A. Migdall would also like to acknowledge DARPA/QuIST support.

## REFERENCES

1. N. Gisin *et al.*, *Rev. Modern Phys.* **74**, 145 (2002).
2. A. Migdall, *Phys. Today* (January, 1999), 41.
3. S. J. van Enk *et al.*, *J. Mod. Opt.* **44**, 1727 (1997); J. I. Cirac, A. K. Ekert, S. F. Huelga, and C. Macchiavello, *Phys. Rev. A* **59**, 4249 (1999); H. Buhrman, R. Cleve, and W. van Dam, *SIAM J. Comput.* **30**, 1829 (2001).
4. E. Knill, R. Laflamme, and G. J. Milburn, *Nature* **409**, 46 (2001).
5. P. Michler *et al.*, *Science* **290**, 2282 (2000); C. Santori *et al.*, *Phys. Rev. Lett.* **86**, 1502 (2001).
6. Z. Yuan *et al.*, *Science* **295**, 102 (2002).
7. J. Vuckovic *et al.*, *Appl. Phys. Lett.* **82**, 3596 (2003); C. Santori *et al.*, *Nature* **419**, 594 (2002).
8. E. Waks *et al.*, *Nature* **420**, 762 (2002); D. Fattal *et al.*, *Phys. Rev. Lett.* **92**, 037903 (2004).
9. M. Pelton *et al.*, *Phys. Rev. Lett.* **89**, 233602 (2002).
10. J. Vuckovic and Y. Yamamoto, *Appl. Phys. Lett.*, **82**, 2374 (2003).
11. L. Brunel, B. Lounis, P. Tamarat, and M. Orrit, *Phys. Rev. Lett.* **83**, 2722 (1999); T.-H. Lee *et al.*, *Phys. Rev. Lett.* **85**, 100 (2004).
12. C. Kurtsiefer, S. Mayer, P. Zarda, and H. Weinfurter, *Phys. Rev. Lett.* **85**, 290 (2000); R. Brouri *et al.*, *Eur. Phys. J. D* **18**, 191 (2002); A. Beveratos *et al.*, *Phys. Rev. Lett.* **89**, 187901 (2002).
13. A. Kuhn, M. Hennrich, and G. Rempe, *Phys. Rev. Lett.* **89**, 067901 (2002); J. McKeever *et al.*, *Science* **303**, 1992 (2004).
14. J. H. Shapiro, *New J. Phys.* **4**, 47.1 (2002).
15. A. Imamoglu, *Phys. Rev. Lett.* **89**, 163602 (2002); D. F. V. James and P. G. Kwiat, *Phys. Rev. Lett.* **89**, 183601 (2002).
16. D. C. Burnham and D. L. Weinberg, *Phys. Rev. Lett.* **25**, 84 (1970).
17. C. K. Hong and L. Mandel, *Phys. Rev. Lett.* **56**, 58 (1986).
18. N. Peters *et al.*, *Quant. Inform and Comput.* **3**, 503–517 (2003); E. Jeffrey, N. A. Peters, and P. G. Kwiat, *New J. Phys.* **6**, 100 (2004).
19. C. Kurtsiefer, M. Oberparleiter, and H. Weinfurter, *Phys. Rev. A* **64**, 023802 (2001); F. A. Bovino *et al.*, *Opt. Commun.* **227**, 343 (2003).
20. S. Takeuchi, *Opt. Lett.* **26**, 843 (2001).
21. A. L. Migdall, D. Branning, and S. Castelletto, *Phys. Rev. A* **66**, 053805 (2002).
22. T. B. Pittman, B. C. Jacobs, and J. D. Franson, *Phys. Rev. A* **66**, 42303 (2002); P. G. Kwiat *et al.*, *Proc. SPIE* **5161**, 87 (2004).
23. P. G. Kwiat *et al.*, *Phys. Rev. Lett.* **75**, 4337 (1995).
24. P. Trojek, Ch. Schmid, M. Bourennane and H. Weinfurter, *Opt. Exp.* **12**, 276 (2004).
25. D. Branning, W. Grice, R. Erdmann, and I. A. Walmsley, *Phys. Rev. A* **62**, 013814 (2000).
26. M. Fiorentino *et al.*, quant-ph/0309071; *Phys. Rev. A* **69**, 041801(R) (2004).
27. P. G. Kwiat *et al.*, *Phys. Rev. A* **60**, R773 (1999).
28. G. Bitton, W. P. Grice, J. Moreau, and L. Zhang *Phys. Rev. A* **65**, 063805 (2002).
29. Y. -H. Kim *et al.*, *Phys. Rev. A* **63**, 062301 (2001).
30. A. G. White, D. F. V. James, P. H. Eberhard, and P. G. Kwiat, *Phys. Rev. Lett.* **83**, 3103 (1999).
31. Y. Nambu *et al.*, *Phys. Rev. A* **66**, 033816 (2002); B.-S. Shi and A. Tomita, *Phys. Rev. A* **69**, 013803 (2004).
32. S. Tanzilli *et al.*, *Electron. Lett.* **37**, 26 (2001); C. E. Kuklewicz *et al.*, *Phys. Rev. A* **69**, 013807 (2004).



33. K. Banaszek, A. B. U'Ren, and I. A. Walmsley, *Opt. Letts.* **26**, 1367 (2001); K. Sanaka, K. Kawahara, and T. Kuga, *Phys. Rev. Lett.* **86**, 5620 (2001).
34. M. Oberparleiter and H. Weinfurter, *Opt. Commun.* **183**, 133 (2000).
35. I. Marcikic *et al.*, *Phys. Rev. A* **66**, 062308 (2002).
36. A. Mair, A. Vaziri, G. Weihs, and A. Zeilinger, *Nature* **412**, 312 (2001); N. K. Langford, quant-ph/0312072.
37. T. B. Pittman *et al.*, in *IEEE J. Selec. Top. Quant. Electron., special issue on "Quantum Internet Technologies"* (2003).
38. M. Fiorentino, P. L. Voss, J. E. Sharping, and P. Kumar, *IEEE Photonics Tech. Lett.* **14**, 983 (2002).
39. X. Li, P. Voss, J. E. Sharping, and P. Kumar, Quant. Electr. and Laser Science Conf., Baltimore, MD, June 1–6, 2003, paper QTuB4 in QELS'03 Technical Digest (Optical Society of America, Washington, D.C. 2003); *ibid*, quant-ph/ 0402191.
40. P. L. Voss and P. Kumar, *Opt. Lett.* **29**, 445 (2004); X. Li, J. Chen, P. Voss, J. Sharping, and P. Kumar, *Opt. Exp.* **12**, 3737 (2004).
41. O. Benson, C. Santori, M. Pelton, and Y. Yamamoto, *Phys. Rev. Lett.* **84**, 2513 (2000).
42. C. Santori *et al.*, *Phys. Rev. B* **66**, 045308 (2002).
43. J. Vuckovic and Y. Yamamoto, *Appl. Phys. Lett.* **82**, 2374 (2003).
44. W. G. Oldham, R. R. Samuelson, and P. Antognetti, *IEEE Trans. Electron. Dev.* **ED-19**, 1056 (1972).
45. <http://optoelectronics.perkinelmer.com/>
46. M. J. Fitch, B. C. Jacobs, T. B. Pittman, and J. D. Franson, *Phys. Rev. A* **68**, 043814 (2003); D. Achilles *et al.*, *Opt. Lett.* **28**, 2387 (2003); J. Rehacek *et al.*, quant-ph/0303032 (2003).
47. E. Waks, K. Inoue, E. Diamanti, and Y. Yamamoto, quant-ph/0308054 (2003).
48. P. G. Kwiat *et al.*, *Appl. Opt.* **33**, 1844 (1994).
49. J. Kim, S. Takeuchi, Y. Yamamoto, and H. H. Hogue, *Appl. Phys. Lett.* **74**, 902 (1999).
50. E. Waks *et al.*, quant-ph/0307162 (2003).
51. A. Lacaita, F. Zappa, S. Cova, and P. Lovati, *Appl. Opt.* **35**, 2986 (1996); G. Ribordy, J.-D. Gautier, H. Zbinden, and N. Gisin, *Appl. Opt.* **37**, 2272 (1998); P. A. Hiskett, G. S. Buller, A. Y. Loudon, J. M. Smith, Ivair Gontijo, Andrew C. Walker, Paul D. Townsend, and Michael J. Robertson, *Appl. Opt.* **39**, 6818 (2000); J. G. Rarity, T. E. Wall, K. D. Ridley, P. C. M. Owens, and P. R. Tapster, *Appl. Opt.* **39**, 6746 (2000); N. Namekata, Y. Makino, S. Inoue, *Opt. Lett.* **27**, 954 (2002); A. Tomita and K. Nakamura, *Opt. Lett.* **27**, 1827 (2002); D. S. Bethune, W. P. Risk, and G. W. Pabst, quant-ph/03111120 (2003); P. L. Voss, K. G. Köprülü, S.-K. Choi, S. Dugan, and P. Kumar, *J. Mod. Opt.* **51**, 1369 (2004).
52. A. Lacaita, P. A. Francese, F. Zappa, and S. Cova, *Appl. Opt.* **33**, 6902 (1994).
53. A. J. Miller, S. W. Nam, J. M. Martinis, and A. V. Sergienko, *Appl. Phys. Lett.* **83**, 791 (2003).
54. A. Peacock *et al.*, *J. Appl. Phys.* **81**, 7641 (1997).
55. G. N. Gol'tsman *et al.*, *Appl. Phys. Lett.* **79**, 705 (2001).
56. M. A. Albota and F. N. C. Wong, *Opt. Lett.* **29**, 1449 (2004).
57. A. P. VanDevender and P. G. Kwiat, *J. Mod. Opt.* **51**, 1433 (2004).
58. K. R. Parameswaran *et al.*, *Opt. Lett.* **27**, 179 (2002).
59. J. M. Huang and P. Kumar, *Phys. Rev. Lett.* **68**, 2153 (1992).
60. "Special Issue: Single-photon: detectors, applications, and measurement methods," A. Migdall and J. Dowling, eds., *J. Mod. Opt.* **51**, 1265–1557 (2004).
61. "Focus Issue: Single photons on demand," P. Grangier, B. Sanders, and J. Vuckovic, eds., *New J. Phys.* **6** (2004). <http://www.iop.org/EJ/abstract/1367-2630/6/1/E04>